

TLRR (Irrc67) interacts with PP1 and is associated with a cytoskeletal complex in the testis

Rong Wang, Aseem Kaul and Ann O. Sperry¹

Department of Anatomy and Cell Biology, Brody School of Medicine at East Carolina University, Greenville, NC 27834, U.S.A.

Background information. Spermatozoa are formed via a complex series of cellular transformations, including acrosome and flagellum formation, nuclear condensation and elongation and removal of residual cytoplasm. Nuclear elongation is accompanied by the formation of a unique cytoskeletal structure, the manchette. We have previously identified a leucine-rich repeat protein that we have named TLRR (testis leucine-rich repeat), associated with the manchette that contains a PP1 (protein phosphatase-1)-binding site. Leucine-rich repeat proteins often mediate protein–protein interactions; therefore, we hypothesize that TLRR acts as a scaffold to link signalling molecules, including PP1, to the manchette near potential substrate proteins important for spermatogenesis.

Results. TLRR and PP1 interact with one another as demonstrated by co-immunoprecipitation and the yeast two-hybrid assay. TLRR binds more strongly to PP1 γ 2 than it does to PP1 α . Anti-phosphoserine antibodies immunoprecipitate TLRR from testis lysate, indicating that TLRR is a phosphoprotein. TLRR is part of a complex in testis that includes cytoskeletal proteins and constituents of the ubiquitin–proteasome pathway. The TLRR complex purified from 3T3 cells contains similar proteins, co-localizes with microtubules and is enriched at the microtubule-organizing centre. TLRR is also detected near the centrosome of elongated, but not mid-stage, spermatids.

Conclusion. We demonstrate here that TLRR interacts with PP1, particularly the testis-specific isoform, PP1 γ 2. Immunoaffinity purification confirms that TLRR is associated with the spermatid cytoskeleton. In addition, proteins involved in protein stability are part of the TLRR complex. These results support our hypothesis that TLRR links signalling molecules to the spermatid cytoskeleton in order to regulate important substrates involved in spermatid transformation. The translocation of TLRR from the manchette to the centrosome region suggests a possible role for this protein in tail formation. Our finding that TLRR is associated with microtubules in cultured cells suggests that TLRR may play a common role in modulating the cytoskeleton in other cell types besides male germ cells.

Introduction

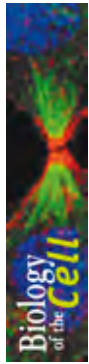
The formation of viable sperm entails a dramatic cytoskeletal rearrangement to transform a rather non-descript precursor cell into a polarized, elongated, free-swimming spermatozoon. During this developmental process, the acrosome forms, the nucleus con-

denses and elongates, the flagellum develops and the cytoplasm redistributes for eventual elimination as a residual body. The manchette is a skirt-like structure comprising a mantle of microtubules attached to a perinuclear ring that encircles the elongating spermatid nucleus during the period of its greatest morphological change (reviewed in Fawcett et al., 1971). The manchette is unique to the developing spermatid and demonstrates several forms of motility by constricting in diameter as it moves along the surface of the spermatid nucleus. In addition, both microtubules and microfilaments of the manchette act as tracks for the transport of vesicles to reallocate cytoplasmic contents for disposal during streamlining of

¹To whom correspondence should be addressed (email sperrya@ecu.edu).

Key words: centrosome, cytoskeleton, leucine-rich repeat, manchette, spermatogenesis, spermiogenesis.

Abbreviations used: CCT, cytoplasmic chaperonin containing TCP-1; DAPI, 4',6-diamidino-2-phenylindole; IC 74.1, intermediate chain 74.1; MALDI, matrix-assisted laser-desorption ionization; MTOC, microtubule-organizing centre; NMIgG, normal mouse IgG; NRIgG, normal rabbit IgG; PP1, protein phosphatase-1; TLRR, testis leucine-rich repeat; TLRRFL, full-length TLRR.



the spermatid in the course of its maturation. Protein complexes are also conveyed along the manchette in a process termed IMT (intramanchette transport) that is thought responsible for the delivery of components to the centrosome and the sperm tail (reviewed in Kierszenbaum, 2002).

Consistent with the observed motility of the manchette, this structure contains both microtubule- and actin-based molecular motors. Kinesin molecular motors are associated with microtubules of the manchette including kinesin-1 (Hall et al., 1992), KIFC1 (a kinesin-13 member) (Yang and Sperry, 2003) and KIF17 β (a kinesin-2 subfamily member) (Saade et al., 2007) as well as cytoplasmic dynein (Hall et al., 1992; Yoshida et al., 1994; Fouquet et al., 2000; Hayasaka et al., 2008). Myosin Va connects vesicles to microfilaments that are interspersed with microtubules of the manchette and is also found in the acroplaxome, a keratin-actin subacrosomal plate (Kierszenbaum et al., 2003; Hayasaka et al., 2008).

Besides molecular motors and cytoskeletal components, additional proteins have been localized to the manchette, an indication of its complex structure and function during spermiogenesis. Signalling molecules such as a testis-specific serine-threonine kinase and the Fer tyrosine kinase have been found associated with manchette microtubules (Walden and Cowan, 1993; Walden and Millette, 1996; Tovich et al., 2004; Kierszenbaum et al., 2008). This placement of kinases is compatible with the proposal that the manchette provides an anchor for signalling molecules to regulate the cellular changes of spermiogenesis (Kierszenbaum, 2001). As expected, proteins involved in cellular remodelling and protein degradation are also linked to the manchette. CCT (cytoplasmic chaperonin containing TCP-1) is a chaperonin responsible for folding of α - and β -tubulin as well as actin and is highly expressed in the testis (Frydman et al., 1992; Gao et al., 1992; Yaffe et al., 1992; Kubota et al., 1999). CCT is localized to the spermatid manchette and to the centrosome, but not to the sperm tail (Soues et al., 2003). The 26S proteasome is also found on the manchette, where it likely functions in the degradation of cytoplasmic contents during spermatid remodelling (Rivkin et al., 1997; Mochida et al., 2000).

We have identified recently a leucine-rich-repeat-containing protein that we have named TLRR [testis leucine-rich repeat; also known as *lrrc67* (leucine-

rich repeat containing 67)] that is highly expressed in the testis and localized near the transforming spermatid nucleus (Wang and Sperry, 2008). In addition to the leucine-rich repeats at its N-terminus, we found a consensus binding site for PP1 (protein phosphatase-1) in the C-terminal half of this protein (Wang and Sperry, 2008). We hypothesize that TLRR may participate in regulating the phosphorylation state of proteins near the spermatid nucleus by localizing PP1 to that site through its association with manchette microtubules. In the present study, we demonstrate the binding of TLRR with PP1 through co-immunoprecipitation from testis lysates and yeast two-hybrid assays. TLRR in the testis exists in a multimeric complex containing cytoskeletal proteins as well as proteins important for protein folding and degradation including CCT and the 26S proteasome, known constituents of the manchette and centrosome in spermatids (Lange et al., 2000; Soues et al., 2003). In mid-stage spermatids, TLRR does not co-localize with γ -tubulin; however, TLRR redistributes to the centrosomal region in late-state spermatids, suggesting a possible role in tail formation. These results support our hypothesis that TLRR positions PP1 near the spermatid nucleus and places this regulatory protein near proteins important for spermiogenesis, including those involved in cytoskeletal remodelling, trafficking and protein degradation.

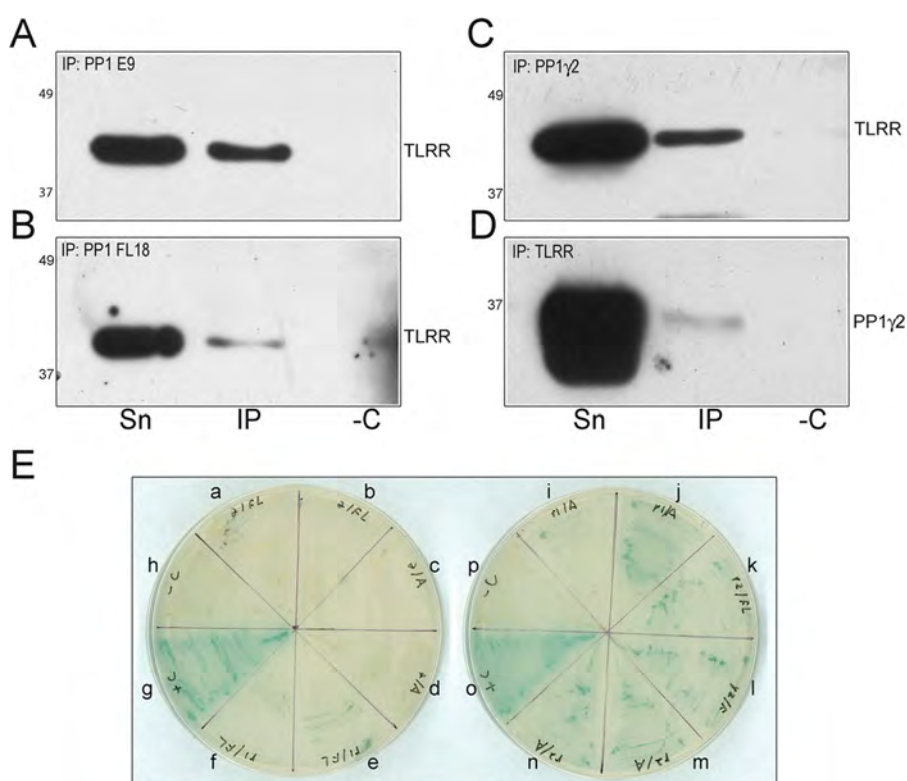
Results

TLRR interacts with PP1 in testis

We previously identified a short amino acid sequence, KVIF, in the C-terminal half of TLRR that matches the consensus binding site for PP1, (R/K)X₁(V/I)X₂(F/W) (Wang and Sperry, 2008). In order to determine whether these two proteins interact in the testis, we performed co-immunoprecipitation studies in testis lysates. Two antibodies that recognize all isoforms of PP1, PP1E9 and PP1FL18, were able to co-immunoprecipitate TLRR (Figures 1A and 1B). In addition, an antibody specific for the γ 2 isoform of PP1 found only in the testis also co-immunoprecipitates TLRR (Figure 1C). In each case a fraction of total TLRR in the testis is complexed with PP1 (compare Sn, representing unbound protein, with IP, corresponding to protein bound to PP1, in each panel). In turn, the TLRR antibody is able to co-immunoprecipitate PP1 γ 2 (Figure 1D);

Figure 1 | TLRR and PP1 interact in the testis

(A–D) Two pan-PP1 antibodies (PP1E9 and PP1FL18), a PP1-isoform-specific antibody (anti-PP1 γ 2) or anti-TLRR, were linked separately to Sepharose beads followed by incubation with 1.5–2 mg of testis lysate. The antibody used for immunoprecipitation is indicated in the upper left-hand side of each panel: (A) PP1E9, (B) PP1FL18, (C) PP1 γ 2 and (D) TLRR. Unbound (Sn) or bound (IP) proteins were separated by PAGE, transferred to a membrane and probed with antibodies directed to the proteins indicated on the right. ‘-C’ indicates proteins bound to Sepharose beads linked to NRIgG as a negative control. The migration of Benchmark prestained protein mass standards (Invitrogen) is indicated on the left of each panel. (E) Yeast two-hybrid interaction assay between TLRR and PP1 isoforms. TLRR, either full-length (TLRRFL) or an N-terminal fragment (TLRRA), and any one of PP1 α , PP1 γ 1 or PP1 γ 2 were co-transformed into the yeast strain YH109. Double transformants were selected on –LEU, –TRP plates and colonies streaked on indicator plates to detect induction of transcription from the LacZ and HIS3 genes. Double transformants shown are (a, b) TLRRFL + PP1 α , (c, d) TLRRA + PP1 α , (e, f) TLRRFL + PP1 γ 1, (i, j) TLRRA + PP1 γ 1, (k, l) TLRRFL + PP1 γ 2 and (m, n) TLRRA + PP1 γ 2. Positive and negative controls for interaction are shown in (g, o) and (h, p) respectively.



however, the percentage of total PP1 γ 2 associated with TLRR in the adult testis is very small. The negative control with NRIgG linked to beads did not precipitate the target proteins.

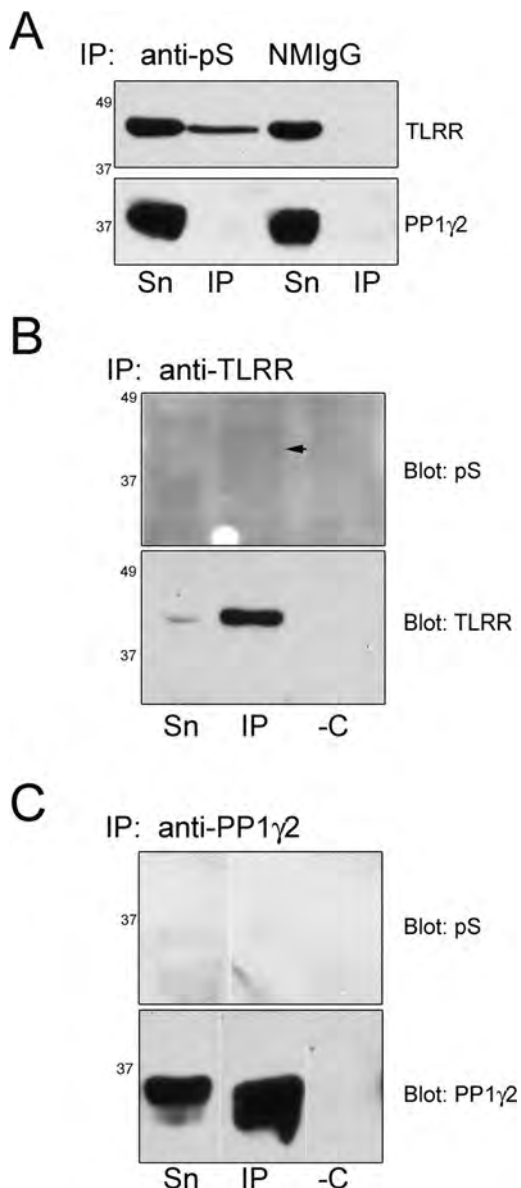
These results strongly suggest that a portion of cellular TLRR exists in the same complex as PP1, but does not establish whether the interaction is direct. In order to explore this possibility, we conducted yeast two-hybrid experiments using yeast expressing TLRRFL (full-length TLRR) in combination with the PP1 isoforms PP1 α , PP1 γ 1 and PP1 γ 2 (Fig-

ure 1E). Colonies containing TLRRFL and PP1 γ 2 (Figures 1Ek and 1El) were blue on selective plates, indicating that these proteins do interact directly with one another. However, their growth was not nearly as robust as that of positive control colonies (Figures 1Eg and 1Eo), indicating either that the interaction between these two proteins is weak or that expression of TLRRFL and/or PP1 inhibits yeast growth. It has been shown previously that PP1 overexpression is deleterious to yeast growth (Liu et al., 1992); the possibility that TLRR might modulate

Figure 2 | TLRR is probably a phosphoprotein

(A) A mixture of mouse anti-phosphoserine antibodies (anti-pS) was linked to Sepharose beads according to the procedure described in the Materials and methods section. NMIgG was linked to beads and used as a negative control for immunoprecipitation. The specificity of the antibody linked to beads is indicated at the top of the panel. Antibody-linked beads were incubated with 1.5–2 mg of testis lysate and unbound (Sn) or bound (IP) proteins were separated by PAGE, transferred to a membrane and probed with the TLRR antibody (upper panel) or the PP1 γ 2 antibody (lower panel). (B) The TLRR antibody bound to Sepharose beads, or (C) the PP1 γ 2-specific antibody linked to beads, was incubated with 1.5–2 mg of testis lysate. Proteins unbound (Sn) or bound to

the beads (IP) were separated by SDS/PAGE, transferred to a membrane and probed first with the anti-phosphoserine antibody (pS), stripped and reprobed with the immunoprecipitating antibody to confirm immunoprecipitation. The arrow in (B) indicates a phosphorylated protein in the bound fraction of the TLRR IP of about the same size as TLRR. PP1 γ 2 does not react with the anti-phosphoserine antibody. The migration of Benchmark prestained protein mass standards (Invitrogen) is indicated on the left.



this effect is currently under investigation. Yeast co-expressing TLRRFL and PP1 γ 1 (Figures 1Ee and 1Ef) were less positive than the TLRRFL/PP1 γ 2 co-transformants, but distinctly more so compared with co-transformants with PP1 α , which were entirely white on indicator plates (Figures 1Ea and 1Eb). These results suggest that interaction between TLRR and PP1 is specific for the γ isoforms and is strongest with PP1 γ 2. Surprisingly, the TLRR construct containing only the first 135 amino acids (TLRRA) and lacking the potential PP1-binding site also appeared blue on indicator plates when co-transformed with PP1 (Figures 1Ei, 1Ej, 1Em and 1En).

TLRR is probably a phosphoprotein

Because TLRR interacts with PP1, we wanted to determine whether it is a candidate substrate for PP1. TLRR contains 12 serine residues with an extremely high probability of phosphorylation using phosphorylation prediction software and only two threonine residues with a modest probability of phosphorylation (Blom et al., 1999) (see Supplementary Figure S1A at <http://www.biocell.org/boc/102/boc1020173add.htm>). Most of the serine residues (9 out of 12) are located in the C-terminal half of the molecule where the PP1-binding site is situated (see Supplementary Figure S1B).

To test whether TLRR might be serine phosphorylated in the testis, we immunoprecipitated proteins from testis lysate using anti-phosphoserine-specific antibodies and probed the immunoprecipitate with the TLRR antibody (Figure 2A, upper panel). A portion of total testicular TLRR is immunoprecipitated with anti-phosphoserine antibodies, making it a potential substrate for PP1 in the testis. When this same blot was probed with the PP1 γ 2-specific antibody, no signal was detected in the immunoprecipitate, even

after overexposure (Figure 2A, lower panel), suggesting that PP1 γ 2 is not phosphorylated in testis lysate at the level of detection afforded by these antibodies and/or PP1 γ 2 that is associated with TLRR is unphosphorylated. The negative control with NMIgG linked to beads did not precipitate TLRR or PP1 γ 2 from testis lysate.

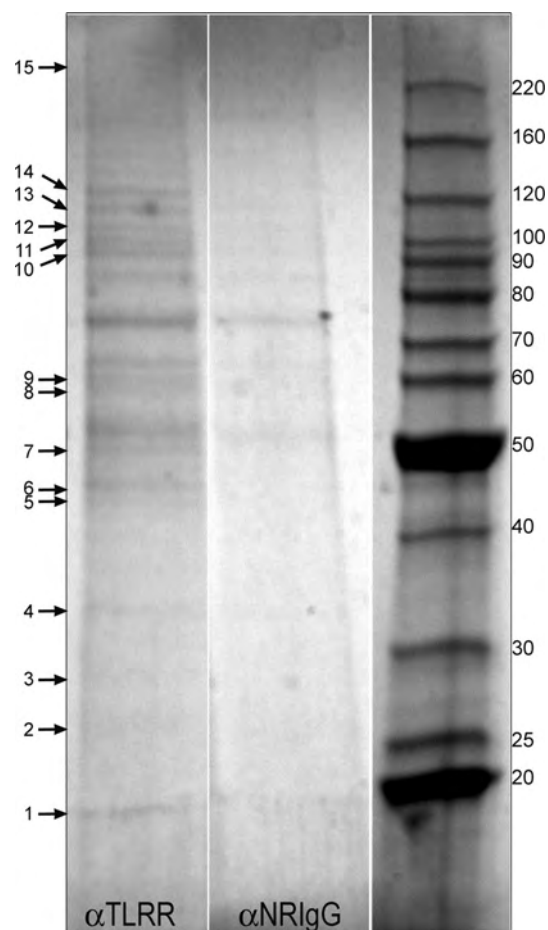
We performed the complementary experiment by immunoprecipitating either TLRR (Figure 2B) or PP1 γ 2 (Figure 2C) from testis lysate and probing the blots with the anti-phosphoserine antibody. In general, the TLRR IP displayed a greater number of reactive bands when compared with the PP1 γ 2 IP, indicating that the TLRR complex may contain a number of phosphorylated proteins. In addition, we confirmed that the target proteins were immunoprecipitated by reprobing each blot with the corresponding immunoprecipitating antibody. Immunoprecipitated TLRR reacts with the phosphoserine antibody (arrow, Figure 2B), whereas immunoprecipitated PP1 γ 2 does not (upper panel, Figure 2C). These results confirm our results given above that TLRR is a phosphoprotein in testis lysate. In addition, neither TLRR nor PP1 γ 2 appears phosphorylated in immunoprecipitates with the partner protein, although this is difficult to discern with regard to PP1 γ 2 co-immunoprecipitated with TLRR because of the relatively high background of the TLRR IP blot.

Proteomic analysis of the TLRR complex

TLRR is found near the spermatid manchette in developing spermatids (Wang and Sperry, 2008); therefore, we reasoned that this protein might be part of a cytoskeletal complex. We conducted a proteomic analysis of the TLRR complex in the testis in an effort to understand the role of TLRR in this tissue. Proteins associated with TLRR were purified from testis lysate using our affinity-purified TLRR antibody linked to Sepharose beads. Bound proteins were eluted from the column, resolved by PAGE and stained with Coomassie Brilliant Blue (Figure 3). A total of 15 protein bands that specifically bound to the TLRR antibody column compared with a control column cross-linked to NRIgG were excised from the gel, sequenced and compared with protein databases. The identified proteins purified with the TLRR antibody can be divided roughly into three categories: cytoskeletal components (Table 1A), proteins

Figure 3 | TLRR is part of a protein complex in the testis containing cytoskeletal proteins, chaperones and components of the protein degradation pathway

An immunoaffinity column was prepared as described in the Materials and methods section and used to purify TLRR and associated proteins from mouse testis lysate. A parallel column was also prepared, linked to NRIgG, as a negative control. Eluates from both columns were concentrated, separated by SDS/PAGE and stained with Coomassie Brilliant Blue R-250. All samples displayed were separated on the same gel. The 15 bands excised for sequencing and identification are numbered on the left and correspond to the numbers listed in Tables 1(A)–1(C). The migration of Benchmark unstained protein mass standards (Invitrogen) is indicated on the right. This experiment was repeated three times, resulting in an identical pattern of TLRR-bound proteins; however, the resolution of the high-molecular-mass band 15 varied with the experiment.



important for regulating protein stability (Table 1B), or miscellaneous metabolic enzymes and other proteins (Table 1C). Each table displays the significant

Table 1 | TLRR is associated with a protein complex containing cytoskeletal proteins, chaperones, components of the ubiquitin-proteasome system and metabolic proteins

Proteins purified by affinity chromatography using a TLRR antibody are grouped into three categories: **(A)** cytoskeletal proteins, both motors and polymer subunits, **(B)** proteins involved in protein stability and **(C)** miscellaneous metabolic proteins and others. The number of peptides, the percentage sequence coverage and the band from which the sequence was derived (shown in Figure 3) are indicated.

(A) Cytoskeletal components

Protein name	Band number	Protein ID	Number of peptides identified	% Sequence coverage	Comments/references
Myosin regulatory light chain Myl9	1	gij198278553	6	45	(Kubalak et al., 1994)
β -Actin	5	Q3UAF7	13	42	(Cleveland et al., 1980)
Kinesin family member 5B	14	Q5BL10	25	29	(Xia et al., 1998)
γ -Actin	1	gij950002	10	27	(Cleveland et al., 1980)
Smooth muscle myosin Myh11	15	gij50510675	42	25	(Matsuoka et al., 1993)
β -Tubulin	7	Q99JZ6	10	24	(Cleveland et al., 1980)
Non-muscle myosin Myh10	15	gij33598964	34	21	(Eddinger and Wolf, 1993)
α -Actin	1	gij49870	6	18	(Cleveland et al., 1980)
Non-muscle myosin Myh9	15	gij114326446	29	18	(Shohet et al., 1989)

(B) Protein stability

Protein name	Band number	Protein ID	Number of peptides identified	% Sequence coverage	Comments/references
Psm3, 26S proteasome non-ATPase subunit 3	8	PSD3_mouse	11	32	(Tanaka and Tsurumi, 1997) manchette associated (Rivkin et al., 1997)
Hsp90 α	10	HS90A	23	29	Highly expressed in testis (Gruppi et al., 1991) proteasome stabilization (Imai et al., 2003)
Psm1, proteasome 26S non-ATPase subunit 1	13	BAE31950	19	25	(Tanaka and Tsurumi, 1997) manchette associated (Rivkin et al., 1997)
Psm2, proteasome 26S non-ATPase subunit 2	11	Q3TWL6	21	24	(Tanaka and Tsurumi, 1997) manchette associated (Rivkin et al., 1997)
Hsp90 β	12	Q91V38	18	22	(Gruppi et al., 1991)
CCT, θ chain	8	JC4073	9	18	Tubulin/actin folding (Gao et al., 1992; Yaffe et al., 1992) manchette associated (Soues et al., 2003)
CCT, γ chain	9	S43062	10	18	Tubulin/actin folding (Gao et al., 1992; Yaffe et al., 1992) manchette associated (Soues et al., 2003)
Hsp4-like	12	AAC52610	14	17	Required for spermatogenesis (Held et al., 2006)
VCP, vasolin-containing protein, AAA (ATPase associated with various cellular activities) ATPase p97	11	S25197	12	14	Ubiquitin pathway (Dai and Li, 2001)
CCT, ζ chain	8	Q52KG9	5	9	Tubulin/actin folding (Gao et al., 1992; Yaffe et al., 1992) manchette associated (Soues et al., 2003)

Table 1 | Continued

(C) Miscellaneous enzymes and other proteins

Protein name	Band number	Protein ID	Number of peptides identified	% Sequence coverage	Comments/references
Glutathione transferase Mu 1	2	gi 6754084	10	49	Metabolism (Hussey and Hayes, 1993)
Peroxiredoxin 6	2	gi 6671549	7	41	Metabolism (Simeone and Phelan, 2005)
Enoyl coA hydratase	3	gi 148685962	8	40	(Ko et al., 2000)
Lactate dehydrogenase c	4	Q64483	9	30	Metabolism, testis-specific isoform, postmeiotic germ cells, required for fertility (Sakai et al., 1987; Odet et al., 2008)
Albumin 1	9	Q546G4	13	21	(Gelly et al., 1994)
MSY2 (Y box protein 2)	6	CAI35155	8	20	Germ cell-specific, mRNA stability, required for spermatogenesis (Gu et al., 1998) (Yang et al., 2007)
Aldose reductase	5	gi 786001	4	12	Metabolism (Spite et al., 2007)
Ilf2 (interleukin enhancer binding factor 2)	6	Q3UXI9	4	10	Transcription, male/female germ cells (López-Fernández and del Mazo, 1996)

matches ($P < 0.05$) in order of percentage sequence coverage and number of peptides identified for each protein.

β -Tubulin, and α -, β - and γ -actin, subunits of cytoskeletal polymers, were purified with the TLRR antibody (Figure 3, bands 7, 1 and 5). In addition to the microtubule-based motor kinesin-1B, actin-based motors are also associated with the TLRR complex. Three isoforms of non-muscle myosin heavy chain, myh11, myh10 and myh9, were affinity-purified with TLRR (Figure 3, band 15). The regulatory light chain 9 is also part of the complex (Figure 3, band 1).

The largest category of proteins associated with TLRR participates in either protein folding or protein degradation (Table 1B). These include three subunits of the CCT (chaperonin containing TCP-1) complex involved in folding of tubulin and actin subunits (Figure 3, bands 8 and 9) (Gao et al., 1992; Yaffe et al., 1992), and Hsp90 (heat-shock protein 90) and Hsp4-like (a member of the Hsp70 family). Another well-represented group associated with the TLRR complex participates in protein degradation including three regulatory subunits of the 26S proteasome (subunits 1, 2 and 3, Figure 3, bands 13, 11 and 8) and VCP (vasolin-containing peptide), required for ubiquitin-proteasome-mediated protein degradation (Dai and

Li, 2001). Our results are consistent with those from other laboratories that localized both the proteasome and CCT to the spermatid manchette (Rivkin et al., 1997; Soues et al., 2003).

Kinesin-1B is associated with TLRR

Tubulin is found in the TLRR complex along with the microtubule-based motor kinesin-1B (Table 1A; Figure 3). A total of 25 peptides matched the kinesin-1B sequence (Table 1A), with some of these peptides overlapping (see Supplementary Figure S2 at <http://www.biolcell.org/boc/102/boc1020173add.htm>). Kinesin-1B is one of three highly homologous isoforms of the kinesin-1 heavy chain expressed in the mouse with different tissue and developmental expression profiles (Aizawa et al., 1992; Vignali et al., 1997; Xia et al., 1998; Kanai et al., 2000; Cai et al., 2001). Therefore we examined the sequence of the peptides and compared them with the published sequence of each isoform. Of the 25 peptides (overbars in Supplementary Figure S2), 19 were exact matches to kinesin-1B sequence with mismatches compared with the A and C isoforms. The six sequences that share common sequences are indicated by an asterisk (Supplementary Figure S2). This is strong evidence that TLRR interacts exclusively with the B isoform of kinesin-1 in testis and not with the A or C isoforms.

Confirmation of cytoskeletal interactions

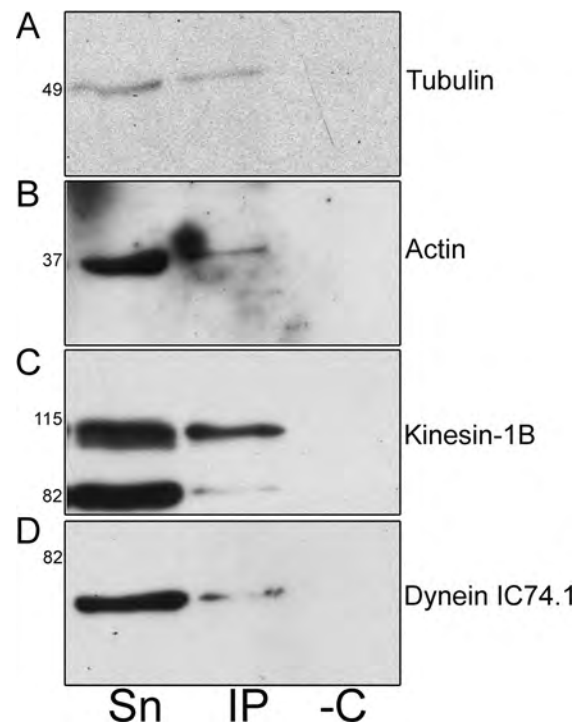
Our proteomic analysis indicated that TLRR resides in a complex containing cytoskeletal polymer subunits and the molecular motor kinesin-1B (see Figure 3 and Table 1A). To confirm and extend these findings, we conducted co-immunoprecipitation experiments of TLRR with cytoskeletal proteins in testis lysates. First, we confirmed that our TLRR antibody could co-immunoprecipitate tubulin and actin from testis lysate, consistent with its localization near the spermatid manchette, a stable cytoskeletal structure composed of microtubules and microfilaments (Figures 4A and 4B). Our proteomic analysis (Table 1A) identified kinesin-1B as associated with TLRR and analysis of the peptides obtained from the tryptic digest (Supplementary Figure S2) confirmed this result. We used an antibody prepared by Dr Scott Brady and his colleagues specific for the B isoform of kinesin-1, UIC 81, to demonstrate that TLRR can co-immunoprecipitate kinesin-1B from testis lysate (Figure 4C) (DeBoer et al., 2008). We also wanted to investigate whether dynein, a minus-end-directed microtubule motor associated with the manchette (Hall et al., 1992; Yoshida et al., 1994; Fouquet et al., 2000; Hayasaka et al., 2008), is co-immunoprecipitated with the TLRR antibody from testis lysate. A fraction of the total population of IC 74.1 (intermediate chain 74.1) of dynein in the testis is found associated with the TLRR antibody (Figure 4D). We also attempted to determine whether myosin Va, shown by others to be associated with the manchette (Kierszenbaum et al., 2003; Hayasaka et al., 2008), immunoprecipitates with TLRR using the dil2 antibody to myosin Va (a gift from Dr J.A. Mercer, McLaughlin Research Institute) (Rogers et al., 1999). However, our results were inconclusive, perhaps because the level of myosin Va in total testis lysate could not be detected by Western blotting with this antibody (R. Wang and A.O. Sperry, unpublished data).

TLRR is expressed in cultured cells in association with microtubules

In the process of transfection studies using TLRR expression vectors, we discovered that several cultured cell lines express the TLRR protein (Figure 5A). We then wanted to determine whether TLRR is associated with microtubules in cultured cells as it

Figure 4 | TLRR interacts with cytoskeletal polymer subunits and molecular motors

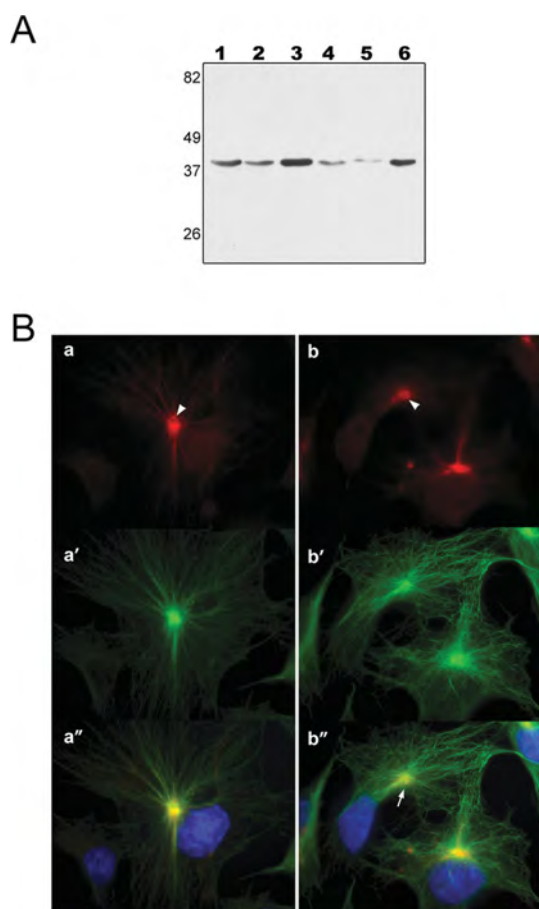
The affinity-purified TLRR antibody bound to Sepharose beads, or non-specific NRIgG (-C), was incubated with 1.5–2 mg of testis lysate. Proteins unbound (Sn) or bound to the beads (IP) were separated by SDS/PAGE, transferred to a membrane and probed with antibodies to the proteins indicated on the right: (A) tubulin, (B) actin, (C) kinesin-1B and (D) dynein IC 74.1. The migration of Benchmark prestained protein mass standards (Invitrogen) is indicated on the left.



is in the testis. Such a finding would provide a malleable system for the investigation of TLRR function in the future. TLRR localizes to the microtubule network in COS7 cells (and 3T3 cells; R. Wang and A.O. Sperry, unpublished data) including the MTOC (microtubule-organizing centre) (Figure 5B). In many cells, we observed that TLRR stained a ring, or loop, around the centre of the MTOC (arrowheads, Figures 5Ba and 5Bb). Interestingly, we observed that, in cells that appeared motile, with a clearly defined leading edge (upper side of Figure 5Bb'), TLRR along with the MTOC was oriented towards the leading edge and displaced from the nucleus (arrow, Figure 5Bb'').

Figure 5 TLRR is expressed in cultured cells and closely aligns with the microtubule cytoskeleton

(A) Protein extracts were made from either mouse testis (lane 1) or cultured cells (lane 2, COS7; lane 3, MCF7; lane 4, DU145; lane 5, C3H-10T1/2; lane 6, NIH 3T3). Protein (100 μ g per well) was loaded, separated by electrophoresis, transferred to a membrane and probed with the TLRR antibody. The migration of Benchmark prestained protein mass standards (Invitrogen) is indicated on the left. **(B)** Two examples of TLRR co-localization with microtubules are shown (a–a'' and b–b''). COS7 cells were grown to approx. 70 % confluency, fixed and double-stained with the TLRR antibody (a, b, red) and an antibody directed to α -tubulin (a', b', green). Arrowheads in (a, b) indicate loops of TLRR antibody-stained material near the MTOC, while the arrow in (b'') indicates the MTOC displaced from the nucleus in a putative motile cell. Signal from the two channels, including the blue channel (DNA, DAPI), was merged in (a'', b''). Scale bar, 10 μ m.



In order to compare the protein composition of the TLRR complex in testis (Table 1) with that in cultured cells, we conducted a proteomic ana-

lysis of the complex purified from 3T3 cell lysate. In this experiment, six bands were excised from a gel containing proteins affinity-purified from 3T3 cell lysate with the TLRR antibody and ten proteins were identified in the complex (see Supplementary Table S1 at <http://www.biocell.org/boc/102/boc1020173add.htm>). The complexes purified from the two cell types contain numerous proteins in common including cytoskeletal proteins and members of the hsp70 and Hsp90 family. In addition, both kinesin-1B and IC 74.1 of dynein co-immunoprecipitated with the anti-TLRR antibody from 3T3 cell lysate (see Supplementary Figure S3 at <http://www.biocell.org/boc/102/boc1020173add.htm>). These results are consistent with a role for TLRR in the structure and/or regulation of the cytoskeleton.

TLRR is associated with the centrosome in late-stage spermatids

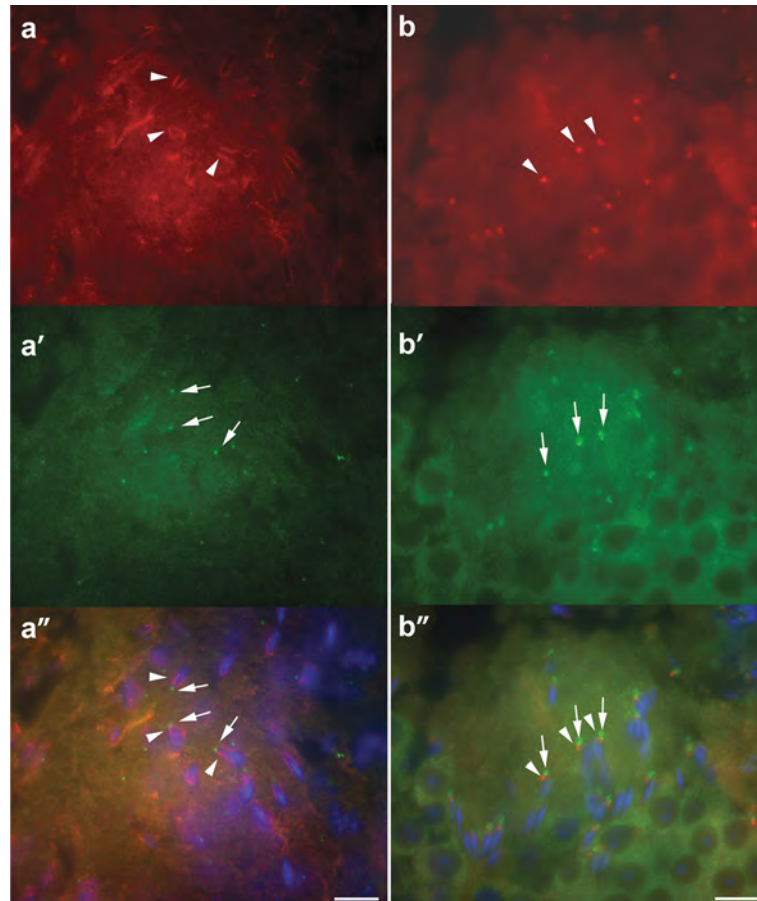
TLRR localizes in part to the MTOC in cultured cells (the present study) and to the nucleus of developing spermatids (arrowheads, Figure 6a; Wang and Sperry, 2008). We next wanted to determine whether the localization of TLRR correlates with the spermatid centriole. Therefore testis sections were double-stained with our TLRR antibody and an antibody to γ tubulin. In mid-stage spermatids, TLRR is localized to the manchette (arrowheads, Figures 6a and 6a'') and does not appreciably co-localize with γ tubulin (arrows, Figures 6a' and 6a''). However, in later-stage spermatids, TLRR localizes to the centrosome region of the elongating spermatid (arrowheads, Figures 6b and b''). At this stage, we routinely observed a bright spot of γ tubulin staining alongside an area of more diffuse staining (arrowheads, Figure 6b'). TLRR staining (arrowheads, Figure 6b'') typically appears just adjacent to the bright spot of γ tubulin staining (arrows, Figure 6b'').

Nocodazole treatment does not completely disrupt TLRR localization

Because TLRR is associated with the microtubule cytoskeleton in cultured cells, we next wanted to determine whether TLRR localization is affected by microtubule depolymerization. COS7 cells were treated with nocodazole to depolymerize microtubules and then the drug was removed and the cells were allowed to recover from drug treatment. Representative

Figure 6 | TLRR localizes to the centrosomal region of late-stage spermatids

Testis sections were triple-stained with antibodies against TLRR (**a**, **b**, red), γ -tubulin (**a'** and **b'**, green) and DAPI (**a''** and **b''**, blue). (**a''**, **b''**) Merged images from all three channels. TLRR staining in mid-stage spermatids (arrowheads, **a** and **a''**) does not align with that of γ -tubulin (arrows, **a'** and **a''**). However, in later-stage spermatids, TLRR (arrowheads, **b** and **b''**) and γ -tubulin (arrows, **b'** and **b''**) are found adjacent to one another in the centrosomal region at the base of the sperm head. Scale bar, 10 μ m.



fluorescent staining of cells for TLRR and tubulin after 0, 60, 120 and 180 min of recovery is shown in Figure 7. In treated cells without recovery, TLRR does not diffuse throughout the cytoplasm, as does tubulin, but remains filamentous in appearance (Figure 7b). In some cells, TLRR staining appeared highly localized at the MTOC (R. Wang and A.O. Sperry, unpublished data); however, the overall organization of TLRR appears more disorganized in treated compared with untreated cells (compare Figure 7b with 5Ba). At 1 h of recovery from nocodazole, short microtubules are observed extending from the MTOC into the cytoplasm (arrows, inset of Figure 7d) with TLRR still filamentous in appearance. By the

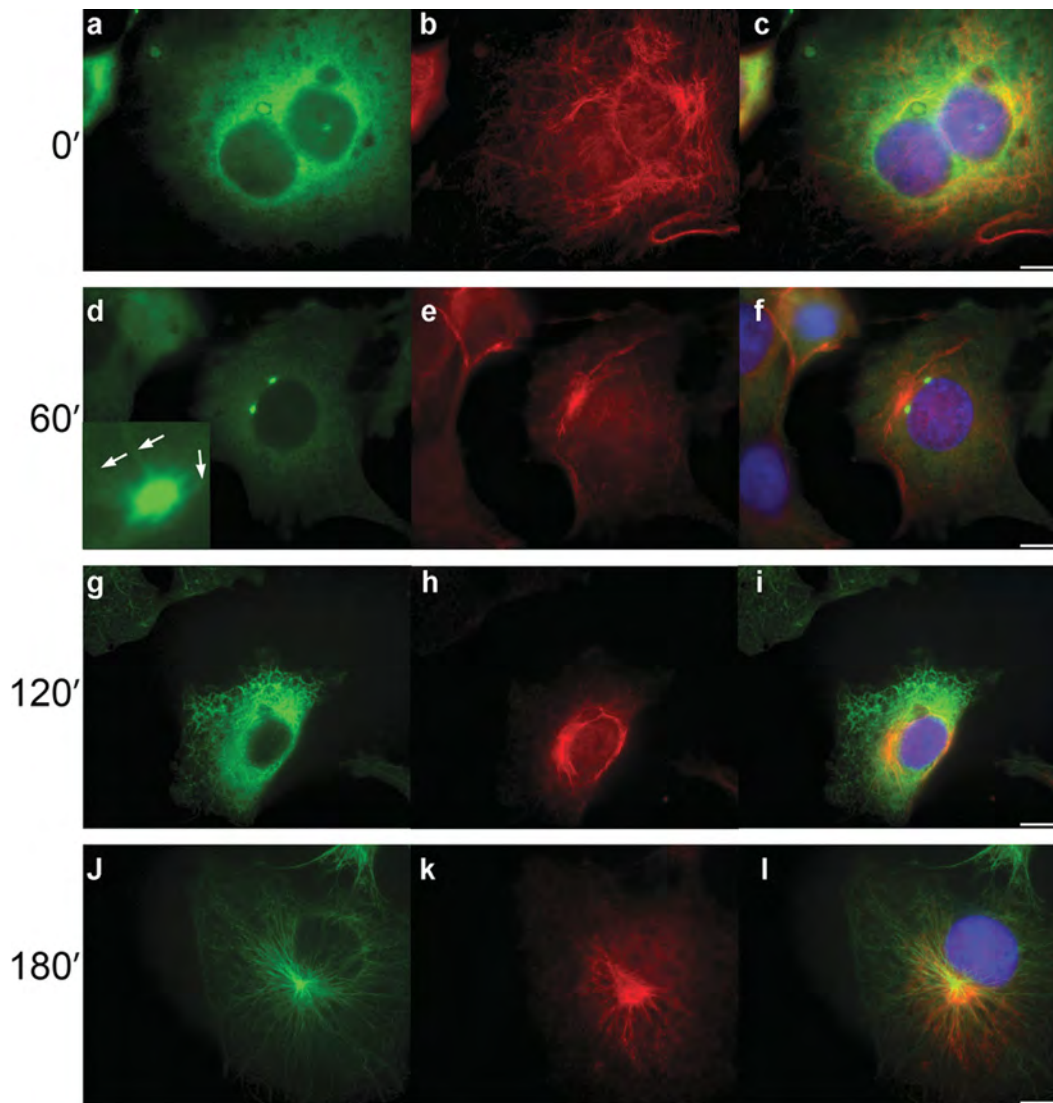
time a normal array of microtubules is apparent at 3 h of recovery, TLRR staining also displays its normal morphology, with strong staining at the MTOC and radial staining along microtubules (Figure 7k). These results suggest that TLRR localization is not entirely dependent on microtubule polymerization.

Discussion

We have shown previously that TLRR is localized near the developing spermatid nucleus and contains four leucine-rich repeats as well as a consensus binding site for PP1 (Wang and Sperry, 2008). In the present paper, we begin to test our hypothesis that

Figure 7 | TLRR localization does not depend entirely on microtubules

COS7 cells were treated with 25 μ M nocodazole for 1.5 h, allowed to recover from drug treatment for 0, 1, 2 or 3 h, fixed and double-stained with anti- α -tubulin (a, d, g, j) and TLRR antibody (b, e, h, k). Respective merged channels for each time point are shown in (c, f, i, l). Scale bar, 10 μ m.



TLRR links PP1 to the spermatid cytoskeleton in order to localize this enzyme near important cellular substrates involved in cellular transformation. To determine whether TLRR interacts with PP1 in the testis, we conducted co-immunoprecipitation experiments in testis lysates. Antibodies that recognize all isoforms of PP1, PP1E9 or PP1FL18, are able to immunoprecipitate the TLRR protein from testis lysate. In addition, we demonstrate that a portion of testicular TLRR is complexed with the testis-specific

isoform of PP1, PP1 γ 2. Yeast two-hybrid assays confirm this interaction and suggest that binding is not solely dependent on the KVIF motif, because interaction still occurs when a TLRR fragment lacking this sequence is used. This is not unusual for PP1 regulatory proteins that often have regions of affinity for PP1 in addition to the consensus binding site (Cohen, 2002). Our interaction studies also indicate a preference for binding between TLRR and PP1 γ 2 compared with PP1 α .

Our present study is consistent with that of Vijayaraghavan and colleagues showing that PP1 γ 2, necessary for sperm motility, is also required for sperm maturation and is localized in developing spermatids as is TLRR (Chakrabarti et al., 2007). These findings, along with our own, support our hypothesis that TLRR, associated with the manchette, brings PP1 near this structure in developing spermatids. sds22, a homologue of TLRR, binds to and inhibits the activity of PP1 γ 2 in caudal, but not caput, spermatozoa (Mishra et al., 2003). The mechanism underlying this inhibition is uncertain; however, it has been proposed that sds22 binding to PP1 γ 2 is regulated by sds22 phosphorylation (Huang et al., 2002; Mishra et al., 2003). We demonstrate here that TLRR is likely a phosphoprotein and speculate that its phosphorylation may also regulate its binding to PP1.

TLRR is localized near the manchette of elongating spermatids, a structure rich in microtubules, microfilaments and associated motor proteins. Therefore we anticipated that the protein complex associated with TLRR would contain cytoskeletal proteins. Our proteomic analysis, and co-immunoprecipitation experiments, revealed that both actin and tubulin are associated with the TLRR complex as well as both microtubule-based and actin-based molecular motors. Our results are similar to those of Cheng et al. (2009) who recently identified a multimeric complex containing PP1 γ 2 and actin along with other proteins in mouse testis lysate. However, PP1 was not identified in our proteomic analysis of the TLRR complex, indicating that its interaction may be transient or small compared with the proteins we detected. Alternatively, PP1 is highly resistant to trypsin digestion, possibly rendering it under-represented in sequence analysis after tryptic digestion (Feng et al., 1991).

Peptide analysis demonstrated that only the B isoform of kinesin-1 is associated with the TLRR complex. Peptides exclusive to kinesin-1B and not the A and C isoforms were detected in the affinity-purified TLRR complex. This result could indicate either that the TLRR complex excludes the A and C isoforms by providing binding sites only for kinesin-1B or that neither A nor C isoform is present in the cell types that express TLRR. Junco et al. (2001) were able to detect all three kinesin-1 isoforms in the testis by RT-PCR (reverse

transcription-PCR), but only the kinesin-1C isoform in spermatids.

In addition, our co-immunoprecipitation experiments demonstrate that the minus-end-directed motor dynein is associated with this complex. Our results suggesting that both plus-end- and minus-end-directed motors are associated with TLRR are consistent with immunofluorescent localization of these motors to the manchette suggested by others and support the idea that the manchette transports cargo in both directions. The interaction of both PP1 and kinesin-1B with TLRR suggests a possible role for TLRR in regulation of kinesin-1B activity associated with the manchette. PP1 is an important regulator of kinesin-based vesicle motility by activation of GSK-3 β (glycogen synthase kinase-3 β), which then phosphorylates the light chain of kinesin, releasing it from its cargo and inhibiting transport (Morfini et al., 2002). Kinesin represents a candidate target on the microtubule manchette for PP1 in association with TLRR.

One of the most intriguing findings from our experiments was the association of numerous non-regulatory subunits of the 26S proteasome with the TLRR complex. This result is consistent with previous immunolocalization of subunits of the proteasome to the spermatid manchette (Rivkin et al., 1997) and supports a role for the manchette in degradation of proteins during sperm maturation. Recently, the proteasome has been implicated in the regulation of microtubule dynamics (Csizmadia et al., 2008; Didier et al., 2008; Poruchynsky et al., 2008); therefore, its localization on the manchette might facilitate a role for the proteasome in controlling the stability of the manchette itself. In addition to subunits of the 26S proteasome, we found Hsp90 associated with the TLRR complex. These results are in accordance with the works of others that demonstrate the necessity of Hsp90 for the assembly and stabilization of the proteasome (Imai et al., 2003).

We previously identified TLRR in a testis cDNA library and demonstrated that it is highly expressed in the testis and localized near the cytoskeleton of developing spermatids (Wang and Sperry, 2008). In the present paper, we report that the TLRR protein is also expressed in many cell lines where it is closely aligned with the microtubule cytoskeleton including the MTOC. Proteomic and co-immunoprecipitation analyses of the TLRR complex in cultured cells

revealed common components including cytoskeletal polymer subunits and Hsps. However, we did not detect proteasome subunits or CCT in the complex from cultured cells, indicating either that our analysis was incomplete or that these protein complexes are preferentially associated with TLRR in the testis. Our results suggest that TLRR may play a common role in cells that can be modulated in specialized cells types, for example in the stable manchette cytoskeletal structure present in developing spermatids.

The behaviour of the centrosome during gametogenesis has been the focus of intense interest based on the importance of establishing an intact spindle to support early divisions of the zygote. In many species, the male and female gametes provide a reciprocal contribution of pericentriolar material (male) and centriole (female) to reconstitute a functional centrosome after fertilization (Manandhar et al., 2005). In the mouse, however, the centrosome undergoes complete degeneration during spermatogenesis (Manandhar et al., 1998). Here, we report that, although TLRR is found on cytoplasmic microtubules and near the MTOC in cultured cells, this protein displays a different distribution during male germ cell development. TLRR is closely associated with the manchette of mid-stage spermatids followed by relocation to the centrosomal region of the spermatid (Figure 6). The relocation of TLRR from the manchette to the centrosome has been observed for a number of other proteins (Kierszenbaum, 2002) including components of the ubiquitin proteasome system (Rivkin et al., 1997, 2009), which we have shown here to be part of the testis TLRR complex.

Expression profiling has recently identified TLRR as a predicted cilia-related gene based on over-expression in highly ciliated cell types such as lung, olfactory epithelium, trachea, testis, and vomeronasal organ (McClintock et al., 2008). In addition, this protein is part of the ciliome database (<http://www.ciliome.com>). This is consistent with our localization of this protein to the MTOC in cultured cells (Figures 5a, 5b and 7k) and near the centrosomal region in spermatids and supports a role for TLRR in microtubule organization and/or biogenesis of cilia/flagella.

The TLRR protein is closely associated with the developing spermatid nucleus. We demonstrate in the present paper that TLRR interacts with PP1 and cytoskeletal proteins as well as proteins important for

the regulation of protein stability and turnover. Our results support our previous immunolocalization of TLRR to the manchette and are consistent with our hypothesis that TLRR serves to link PP1, and other regulatory molecules, near the nucleus of developing male germ cells in order to guide proper cell transformation.

Materials and methods

Co-immunoprecipitation

All use of animals was approved and conducted in accordance with the Guide for the Care and Use of Agricultural Animals in Agricultural Research and Teaching. Mouse testis extract was prepared as described previously (Zou et al., 2002). Briefly, decapsulated testes from adult mice were homogenized in a buffer [10 mM Mes, pH 6.75, 1 mM EGTA, 0.5 mM MgCl₂, 30% (v/v) glycerol and 0.1% Nonidet P40] containing mammalian protease inhibitor cocktail (Sigma–Aldrich, St. Louis, MO, U.S.A.), 3 μM PMSF and phosphatase inhibitor cocktail (Sigma–Aldrich), centrifuged twice, first at 100 000 g and then at 130 000 g, to remove cellular debris, generating a high-speed supernatant fraction. The protein concentration in tissue lysates was determined by the Coomassie Brilliant Blue method (Bio-Rad Laboratories, Hercules, CA, U.S.A.). For co-immunoprecipitation experiments, affinity-purified antibody directed to either TLRR or PP1γ2 was linked to CNBr-activated Sepharose 4B (GE Healthcare, Pittsburgh, PA, U.S.A.) according to the manufacturer's instructions. Testis lysate (1.5–2 mg of protein) was incubated with antibody-linked Sepharose beads overnight at 4°C. Immune complexes were collected by centrifugation, unbound protein was removed and the pellet was washed extensively to remove non-specifically bound protein. Bound proteins were then eluted from the pellet with triethanolamine (pH 11) and denatured, proteins were separated by SDS/PAGE and bound proteins were detected by Western blotting. Negative control for co-immunoprecipitation with TLRR or PP1 antibodies was NRIgG (normal rabbit IgG) bound to beads. For experiments to determine whether TLRR or PP1γ2 is phosphorylated, the testis extract was incubated with Sepharose beads linked to 12 μg of anti-phosphoserine antibodies (a mixture of clones 1CB, 4A3, 4A9 and 16B3 from EMD Chemical, Gibbstown, NJ, U.S.A.) or control beads linked to an equivalent amount of NMIgG (normal mouse IgG).

Yeast two-hybrid analysis

Plasmids containing coding sequence for PP1γ1 and PP1γ2 were gifts from Dr S. Vijayaraghavan (Department of Biological Sciences, Kent State University, Kent, OH, U.S.A.). Both sequences were amplified by PCR before transfer into pGBKT7 using BamHI and EcoRI restriction sites engineered into the PCR primers. PP1γ1 was amplified with GAATTCGCGGATATCGACAAACTCAAC as the 5' primer and GGATCCTTTCTTTGCTTGCTTTGTGATC as the 3' primer, while PP1γ2 was amplified with the same 5' primer as for PP1γ1 and GGATCCCTCGTATAGGACCAGTGTG as the 3' primer. PP1α cloned into pGBKT7 was a gift from Dr Susannah Varmuza (Department of Cell and System Biology,

University of Toronto, Toronto, Ontario, Canada). Full-length TLRR cloned into pADT7 and the deletion construct TLRR Δ containing only the first 135 amino acids of TLRR and lacking the KVIF consensus binding site for PP1 were described previously (Wang and Sperry, 2008). The bait (PP1) and prey (TLRR) plasmids were co-transformed into the yeast strain AH109 and activation of the *LacZ* and *HIS3* reporter genes was determined by growth on selective plates containing X- α -Gal as described (Zhang et al., 2007). The yeast strain AH109 (Clontech, Palo Alto, CA, U.S.A.) co-transformed with pGADT7-T and pGBKT7-53 was used as a positive control for protein-protein interaction, while cells containing pGADT7-T and pGBKT7-Lam, expressing proteins that do not interact, were negative controls for these experiments.

Western blotting

Protein samples from immunoprecipitation experiments or affinity purification fractions were separated by PAGE through 10% acrylamide gels or precast 8–16% acrylamide gels (Invitrogen, Carlsbad, CA, U.S.A.), equilibrated in and electrophoretically transferred from the gel matrix to a PVDF membrane (Bio-Rad Laboratories) in Towbin transfer buffer (25 mM Tris base, 1.92 M glycine and 15% methanol). Proteins were detected on the membrane with affinity-purified TLRR antibody prepared as previously described at a dilution of 1:5000 (Wang and Sperry, 2008). Other antibodies used for Western blotting in these experiments were the pan-PP1 antibodies PP1FL18 and PP1E9 (both at 1:250; Santa Cruz Biotechnology, Santa Cruz, CA, U.S.A.), anti-PP1 γ 2 (1:5000; a gift from Dr S. Vijayaraghavan) (Vijayaraghavan et al., 1996), anti- β -tubulin (1:1000; Sigma-Aldrich), anti-actin (20–33, Sigma-Aldrich), UIC 81 specific for kinesin-1B (1:250; a gift from Dr Scott Brady, Department of Anatomy and Cell Biology, University of Illinois, Chicago, IL, U.S.A.) (DeBoer et al., 2008), anti-actin (20–33) (1:200; Sigma-Aldrich), IC 74.1 of dynein (1:250; a gift from Dr K. Pfister, Department of Cell Biology, University of Virginia, Charlottesville, VA, U.S.A.) (Dillman and Pfister, 1994). Immune complexes bound to the membrane were detected with horseradish-peroxidase-conjugated donkey secondary antibody (Jackson ImmunoResearch Laboratories, West Grove, PA, U.S.A.) diluted 1:40000 in TTBS (100 mM Tris, pH 7.5, 150 mM NaCl and 0.1% Tween 20) and developed with ECL reagents as described by the manufacturer (GE Healthcare).

Immunoaffinity purification

A concentrated TLRR antibody stock (approx. 5 mg/ml) was prepared by affinity purification using the antigenic peptide linked to CNBr-activated Sepharose 4B according to the manufacturer's instructions. An affinity purification column was prepared essentially according to the method of Huang et al. (2002) and adapted from that described by Ausubel (1987). The 1 ml column was equilibrated in ice-cold TSA buffer (10 mM Tris/HCl, pH 8.2, 140 mM NaCl and 0.025% NaN₃) supplemented with protease and phosphatase inhibitors. Approx. 20–50 mg of testis lysate in 1.0 ml of TSA was loaded on to the column and incubated, with gentle mixing, overnight at 4°C. The column was then washed sequentially with 5 bed vol. of each of the following buffers: wash 1 (10 mM Tris, pH 8.0, 140 mM NaCl, 0.5% Triton X-100 and 0.5% sodium deoxycholate), wash 2 (50 mM

Tris, pH 8.0, 0.5 M NaCl and 0.1% Triton X-100) and wash 3 (50 mM Tris, pH 9.0, 0.5 M NaCl and 0.1% Triton X-100) and the flow-through was collected. Bound complexes were eluted from the column with 2.5 ml of elution buffer (50 mM triethanolamine, pH 11.5, 0.1% Triton X-100 and 0.15 M NaCl) and fractions were immediately neutralized with 1 M Tris (pH 6.7). A parallel negative control column was prepared with an equal amount of non-specific antibody NRIgG linked to Sepharose and loaded and eluted identically with the experimental sample. Column eluates were concentrated 20–30-fold on an Amicon ultra-4 filter unit (Millipore, Billerica, MA, U.S.A.) prior to analysis by SDS/PAGE.

Proteomic analysis

Proteins eluted from affinity columns were separated by electrophoresis on precast 8–16% acrylamide gels (Invitrogen). Gels were fixed in 25% propan-2-ol/10% acetic acid for 20 min, stained with 0.01% Coomassie Brilliant Blue R-250 (Bio-Rad Laboratories) and destained with 10% acetic acid. Stained bands, not present in the negative control, were excised, and proteins were digested in gel with trypsin and identified by MALDI (matrix-assisted laser-desorption ionization)-TOF (time-of-flight)/TOF and MALDI mass 'fingerprinting' and database search by the UNC-Duke Michael Hooker Proteomics Center (University of North Carolina-Chapel Hill, Chapel Hill, NC, U.S.A.). Kinesin-1 sequences (1A accession number NM_008447, 1B accession number NM_008448 and 1C accession number NM_008449) were aligned using ClustalW2 alignment software (Larkin et al., 2007) and printout was prepared using the Boxshade program.

Co-localization

TLRR was detected in cultured cells essentially as previously described (Yang and Sperry, 2003). COS7 cells were grown to approx. 70% confluence on coverslips, fixed and permeabilized with acetone/methanol (1:1, v/v) or 100% methanol at -20°C for 10 min, and blocked in 2% (w/v) BSA in TBST (20 mM Tris, pH 7.5, 154 mM NaCl, 2 mM EGTA, 2 mM MgCl₂ and 0.1% Triton X-100) for 30 min. The cells were incubated with TLRR polyclonal antibody diluted 1:50 in TBST (approx. 100 μ g/ml) overnight at 4°C. The TLRR polyclonal antibody was detected with a Texas Red-conjugated donkey anti-rabbit IgG secondary antibody (1:100 dilution; Jackson ImmunoResearch Laboratories) and tubulin was detected with an FITC-conjugated monoclonal anti- α -tubulin antibody (1:200; Sigma-Aldrich). DNA was stained with DAPI (4',6-diamidino-2-phenylindole) incorporated into Vectashield mounting medium (Vector Laboratories, Burlingame, CA, U.S.A.). In certain experiments, 2.5 μ g/ml nocodazole was added to the culture medium in order to depolymerize microtubules. After 1.5 h of treatment, the medium was replaced with fresh medium lacking nocodazole, incubated for 1, 2 or 3 h and the cells were fixed and double-stained for TLRR and tubulin as described above.

For co-localization in testis sections, testes obtained from sexually mature mice were immersion-fixed overnight in 4% (w/v) PFA (paraformaldehyde) in PBS (pH 7.4) after piercing of the capsule. The organs were then incubated overnight in 0.5 M sucrose in PBS, placed in a cryoprotectant, cut into 10 μ m sections, transferred to Vectabond-coated slides (Vector

Laboratories), quickly dipped in -20°C acetone and allowed to dry. The sections were washed with PBS and treated with 0.3% Triton X-100 for 15 min at room temperature (22°C). The tissue was blocked in 2% BSA in TBST and incubated with TLRR polyclonal antibody diluted 1:50 in TBST and anti- γ -tubulin diluted 1:50 (clone GTU-88, Sigma–Aldrich). TLRR was detected as described above for co-localization in cultured cells and γ -tubulin was detected with mouse anti- γ -tubulin conjugated to FITC (1:100 dilution; Jackson ImmunoResearch Laboratories). The intracellular localization of proteins was observed with a Nikon E600 fluorescence microscope, Pan Fluor $\times 100$ objective [NA (numerical aperture) 0.5–1.3], fitted with appropriate filters and images were captured with an Orca II CCD camera (charge-coupled-device camera), model C4742-95 (Hamamatsu, Bridgewater, NJ, U.S.A.), and Metamorph image analysis and acquisition software (Universal Imaging Corporation, Downingtown, PA, U.S.A.). Images were exported to Photoshop and only linear adjustments to brightness and/or contrast were performed.

Acknowledgement

We acknowledge the technical assistance of Nicole DeVaul.

Funding

This work was supported by the Division of Research and Graduate Studies, East Carolina University; and the National Institutes of Health [grant number HD058027] (to A.O.S).

References

- Aizawa, H., Sekine, Y., Takemura, R., Zhang, Z., Nangaku, M. and Hirokawa, N. (1992) Kinesin family in murine central nervous system. *J. Cell Biol.* **119**, 1287–1296
- Ausubel, F.M. (1987) *Current Protocols in Molecular Biology*, John Wiley and Sons, New York
- Blom, N., Gammeltoft, S. and Brunak, S. (1999) Sequence and structure-based prediction of eukaryotic protein phosphorylation sites. *J. Mol. Biol.* **294**, 1351–1362
- Cai, Y., Singh, B.B., Aslanukov, A., Zhao, H. and Ferreira, P.A. (2001) The docking of kinesins, KIF5B and KIF5C, to Ran-binding Protein 2 (RanBP2) is mediated via a novel RanBP2 domain. *J. Biol. Chem.* **276**, 41594–41602
- Chakrabarti, R., Kline, D., Lu, J., Orth, J., Pilder, S. and Vijayaraghavan, S. (2007) Analysis of Ppp1cc-null mice suggests a role for PP1 γ 2 in sperm morphogenesis. *Biol. Reprod.* **76**, 992–1001
- Cheng, L., Pilder, S., Nairn, A.C., Ramdas, S. and Vijayaraghavan, S. (2009) PP1 γ 2 and PPP1R11 are parts of a multimeric complex in developing testicular germ cells in which their steady state levels are reciprocally related. *PLoS ONE* **4**, e4861
- Cleveland, D.W., Lopata, M.A., MacDonald, R.J., Cowan, N.J., Rutter, W.J. and Kirschner, M.W. (1980) Number and evolutionary conservation of alpha- and beta-tubulin and cytoplasmic beta- and gamma-actin genes using specific cloned cDNA probes. *Cell* **20**, 95–105
- Cohen, P.T. (2002) Protein phosphatase 1 – targeted in many directions. *J. Cell Sci.* **115**, 241–256
- Csizmadia, V., Raczynski, A., Csizmadia, E., Fedyk, E.R., Rottman, J. and Alden, C.L. (2008) Effect of an experimental proteasome inhibitor on the cytoskeleton, cytosolic protein turnover, and induction in the neuronal cells *in vitro*. *Neurotoxicology* **29**, 232–243
- Dai, R.M. and Li, C.C. (2001) Valosin-containing protein is a multi-ubiquitin chain-targeting factor required in ubiquitin-proteasome degradation. *Nat. Cell Biol.* **3**, 740–744
- DeBoer, S.R., You, Y., Szodorai, A., Kaminska, A., Pignino, G., Nwabuisi, E., Wang, B., Estrada-Hernandez, T., Kins, S., Brady, S.T. and Morfini, G. (2008) Conventional kinesin holoenzymes are composed of heavy and light chain homodimers. *Biochemistry* **47**, 4535–4543
- Didier, C., Merdes, A., Gairin, J.E. and Jabrane-Ferrat, N. (2008) Inhibition of proteasome activity impairs centrosome-dependent microtubule nucleation and organization. *Mol. Biol. Cell* **19**, 1220–1229
- Dillman, III, J.F. and Pfister, K.K. (1994) Differential phosphorylation *in vivo* of cytoplasmic dynein associated with anterogradely moving organelles. *J. Cell Biol.* **127**, 1671–1681
- Eddinger, T.J. and Wolf, J.A. (1993) Expression of four myosin heavy chain isoforms with development in mouse uterus. *Cell Motil. Cytoskeleton* **25**, 358–368
- Fawcett, D.W., Anderson, W.A. and Phillips, D.M. (1971) Morphogenetic factors influencing the shape of the sperm head. *Dev. Biol.* **26**, 220–251
- Feng, Z.H., Wilson, S.E., Peng, Z.Y., Schlender, K.K., Reimann, E.M. and Trumbly, R.J. (1991) The yeast GLC7 gene required for glycogen accumulation encodes a type1 protein phosphatase. *J. Biol. Chem.* **266**, 23796–23801
- Fouquet, J., Kann, M., Soues, S. and Melki, R. (2000) ARP1 in Golgi organisation and attachment of manchette microtubules to the nucleus during mammalian spermatogenesis. *J. Cell Sci.* **113**, 877–886
- Frydman, J., Nimmesgern, E., Erdjument-Bromage, H., Wall, J.S., Tempst, P. and Hartl, F.U. (1992) Function in protein folding of TRiC, a cytosolic ring complex containing TCP-1 and structurally related subunits. *EMBO J.* **11**, 4767–4778
- Gao, Y., Thomas, J.O., Chow, R.L., Lee, G.H. and Cowan, N.J. (1992) A cytoplasmic chaperonin that catalyzes beta-actin folding. *Cell* **69**, 1043–1050
- Gelly, J.L., Richoux, J.P. and Grignon, G. (1994) Immunolocalization of albumin and transferrin in germ cells and Sertoli cells during rat gonadal morphogenesis and postnatal development of the testis. *Cell Tissue Res.* **276**, 347–351
- Gruppi, C.M., Zakeri, Z.F. and Wolgemuth, D.J. (1991) Stage and lineage-regulated expression of two hsp90 transcripts during mouse germ cell differentiation and embryogenesis. *Mol. Reprod. Dev.* **28**, 209–217
- Gu, W., Tekur, S., Reinbold, R., Eppig, J.J., Choi, Y.C., Zheng, J.Z., Murray, M.T. and Hecht, N.B. (1998) Mammalian male and female germ cells express a germ cell-specific Y-box protein, MSY2. *Biol. Reprod.* **59**, 1266–1274
- Hall, E.S., Eveleth, J., Jiang, C., Redenbach, D.M. and Boekelheide, K. (1992) Distribution of the microtubule-dependent motors cytoplasmic dynein and kinesin in rat testis. *Biol. Reprod.* **46**, 817–828
- Hayasaka, S., Terada, Y., Suzuki, K., Murakawa, H., Tachibana, I., Sankai, T., Murakami, T., Yaegashi, N. and Okamura, K. (2008) Intramanchette transport during primate spermiogenesis: expression of dynein, myosin Va, motor recruiter myosin Va, VIIa-Rab27a/b interacting protein, and Rab27b in the manchette during human and monkey spermiogenesis. *Asian J. Androl.* **10**, 561–568

- Held, T., Paprotta, I., Khulan, J., Hemmerlein, B., Binder, L., Wolf, S., Schubert, S., Meinhardt, A., Engel, W. and Adham, I.M. (2006) Hspa4l-deficient mice display increased incidence of male infertility and hydronephrosis development. *Mol. Cell. Biol.* **26**, 8099–8108
- Huang, Z., Khatra, B., Bollen, M., Carr, D.W. and Vijayaraghavan, S. (2002) Sperm PP1gamma2 is regulated by a homologue of the yeast protein phosphatase binding protein sds22. *Biol. Reprod.* **67**, 1936–1942
- Hussey, A.J. and Hayes, J.D. (1993) Human Mu-class glutathione S-transferases present in liver, skeletal muscle and testicular tissue. *Biochim. Biophys. Acta* **1203**, 131–141
- Imai, J., Maruya, M., Yashiroda, H., Yahara, I. and Tanaka, K. (2003) The molecular chaperone Hsp90 plays a role in the assembly and maintenance of the 26S proteasome. *EMBO J.* **22**, 3557–3567
- Junco, A., Bhullar, B., Tarnasky, H.A. and van der Hoorn, F.A. (2001) Kinesin light-chain KLC3 expression in testis is restricted to spermatids. *Biol. Reprod.* **64**, 1320–1330
- Kanai, Y., Okada, Y., Tanaka, Y., Harada, A., Terada, S. and Hirokawa, N. (2000) KIF5C, a novel neuronal kinesin enriched in motor neurons. *J. Neurosci.* **20**, 6374–6384
- Kierszenbaum, A.L. (2001) Spermatid manchette: plugging proteins to zero into the sperm tail. *Mol. Reprod. Dev.* **59**, 347–349
- Kierszenbaum, A.L. (2002) Intramanchette transport (IMT): managing the making of the spermatid head, centrosome, and tail. *Mol. Reprod. Dev.* **63**, 1–4
- Kierszenbaum, A.L., Rivkin, E. and Tres, L.L. (2003) The actin-based motor myosin Va is a component of the acroplaxome, an acrosome-nuclear envelope junctional plate, and of manchette-associated vesicles. *Cytogenet. Genome Res.* **103**, 337–344
- Kierszenbaum, A.L., Rivkin, E. and Tres, L.L. (2008) Expression of FerT testis (FerT) tyrosine kinase transcript variants and distribution sites of FerT during the development of the acrosome-acroplaxome-manchette complex in rat spermatids. *Dev. Dyn.* **237**, 3882–3891
- Ko, M.S., Kitchen, J.R., Wang, X., Threat, T.A., Wang, X., Hasegawa, A., Sun, T., Grahovac, M.J., Kargul, G.J., Lim, M.K. et al. (2000) Large-scale cDNA analysis reveals phased gene expression patterns during preimplantation mouse development. *Development* **127**, 1737–1749
- Kubalak, S.W., Miller-Hance, W.C., O'Brien, T.X., Dyson, E. and Chien, K.R. (1994) Chamber specification of atrial myosin light chain-2 expression precedes septation during murine cardiogenesis. *J. Biol. Chem.* **269**, 16961–16970
- Kubota, H., Yokota, S., Yanagi, H. and Yura, T. (1999) Structures and co-regulated expression of the genes encoding mouse cytosolic chaperonin CCT subunits. *Eur. J. Biochem.* **262**, 492–500
- Lange, B.M., Bachi, A., Wilm, M. and Gonzalez, C. (2000) Hsp90 is a core centrosomal component and is required at different stages of the centrosome cycle in *Drosophila* and vertebrates. *EMBO J.* **19**, 1252–1262
- Larkin, M.A., Blackshields, G., Brown, N.P., Chenna, R., McGettigan, P.A., McWilliam, H., Valentin, F., Wallace, I.M., Wilm, A., Lopez, R. et al. (2007) Clustal W and Clustal X version 2.0. *Bioinformatics* **23**, 2947–2948
- Liu, H., Krizek, J. and Bretscher, A. (1992) Construction of a GAL1-regulated yeast cDNA expression library and its application to the identification of genes whose overexpression causes lethality in yeast. *Genetics* **132**, 665–673
- López-Fernández, L. and del Mazo, J. (1996) Characterization of genes expressed early in mouse spermatogenesis, isolated from a subtractive cDNA library. *Mamm. Genome* **7**, 698–700
- Manandhar, G., Sutovsky, P., Joshi, H.C., Stearns, T. and Schatten, G. (1998) Centrosome reduction during mouse spermiogenesis. *Dev. Biol.* **203**, 424–434
- Manandhar, G., Schatten, H. and Sutovsky, P. (2005) Centrosome reduction during gametogenesis and its significance. *Biol. Reprod.* **72**, 2–13
- Matsuoka, R., Yoshida, M.C., Furutani, Y., Imamura, S., Kanda, N., Yanagisawa, M., Masaki, T. and Takao, A. (1993) Human smooth muscle myosin heavy chain gene mapped to chromosomal region 16q12. *Am. J. Med. Genet.* **46**, 61–67
- McClintock, T.S., Glasser, C.E., Bose, S.C. and Bergman, D.A. (2008) Tissue expression patterns identify mouse cilia genes. *Physiol. Genom.* **32**, 198–206
- Mishra, S., Somanath, P.R., Huang, Z. and Vijayaraghavan, S. (2003) Binding and inactivation of the germ cell-specific protein phosphatase PP1gamma2 by sds22 during epididymal sperm maturation. *Biol. Reprod.* **69**, 1572–1579
- Mochida, K., Tres, L.L. and Kierszenbaum, A.L. (2000) Structural features of the 26S proteasome complex isolated from rat testis and sperm tail. *Mol. Reprod. Dev.* **57**, 176–184
- Morfini, G., Szebenyi, G., Elluru, R., Ratner, N. and Brady, S.T. (2002) Glycogen synthase kinase 3 phosphorylates kinesin light chains and negatively regulates kinesin-based motility. *EMBO J.* **21**, 281–293
- Odet, F., Duan, C., Willis, W.D., Goulding, E.H., Kung, A., Eddy, E.M. and Goldberg, E. (2008) Expression of the gene for mouse lactate dehydrogenase C (Ldhc) is required for male fertility. *Biol. Reprod.* **79**, 26–34
- Poruchynsky, M.S., Sackett, D.L., Robey, R.W., Ward, Y., Annunziata, C. and Fojo, T. (2008) Proteasome inhibitors increase tubulin polymerization and stabilization in tissue culture cells: a possible mechanism contributing to peripheral neuropathy and cellular toxicity following proteasome inhibition. *Cell Cycle* **7**, 940–949
- Rivkin, E., Cullinan, E.B., Tres, L.L. and Kierszenbaum, A.L. (1997) A protein associated with the manchette during rat spermiogenesis is encoded by a gene of the TBP-1-like subfamily with highly conserved ATPase and protease domains. *Mol. Reprod. Dev.* **48**, 77–89
- Rivkin, E., Kierszenbaum, A.L., Gil, M. and Tres, L.L. (2009) Rnf19a, a ubiquitin protein ligase, and Psmc3, a component of the 26S proteasome, tether to the acrosome membranes and the head-tail coupling apparatus during rat spermatid development. *Dev. Dyn.* **238**, 1851–1861
- Rogers, S.L., Karcher, R.L., Roland, J.T., Minin, A.A., Steffen, W. and Gelfand, V.I. (1999) Regulation of melanosome movement in the cell cycle by reversible association with myosin V. *J. Cell Biol.* **146**, 1265–1276
- Saade, M., Irla, M., Govin, J., Victorero, G., Samson, M. and Nguyen, C. (2007) Dynamic distribution of spatial during mouse spermatogenesis and its interaction with the kinesin KIF17b. *Exp. Cell Res.* **313**, 614–626
- Sakai, I., Sharief, F.S. and Li, S.S. (1987) Molecular cloning and nucleotide sequence of the cDNA for sperm-specific lactate dehydrogenase-C from mouse. *Biochem. J.* **242**, 619–622
- Shohet, R.V., Conti, M.A., Kawamoto, S., Preston, Y.A., Brill, D.A. and Adelstein, R.S. (1989) Cloning of the cDNA encoding the myosin heavy chain of a vertebrate cellular myosin. *Proc. Natl. Acad. Sci. U.S.A.* **86**, 7726–7730
- Simeone, M. and Phelan, S.A. (2005) Transcripts associated with Prdx6 (peroxiredoxin 6) and related genes in mouse. *Mamm. Genome* **16**, 103–111
- Soues, S., Kann, M.L., Fouquet, J.P. and Melki, R. (2003) The cytosolic chaperonin CCT associates to cytoplasmic microtubular structures during mammalian spermiogenesis and to heterochromatin in germline and somatic cells. *Exp. Cell Res.* **288**, 363–373

- Spite, M., Baba, S.P., Ahmed, Y., Barski, O.A., Nijhawan, K., Petrash, J.M., Bhatnagar, A. and Srivastava, S. (2007) Substrate specificity and catalytic efficiency of aldo-keto reductases with phospholipid aldehydes. *Biochem. J.* **405**, 95–105
- Tanaka, K. and Tsurumi, C. (1997) The 26S proteasome: subunits and functions. *Mol. Biol. Rep.* **24**, 3–11
- Tovich, P.R., Sutovsky, P. and Oko, R.J. (2004) Novel aspect of perinuclear theca assembly revealed by immunolocalization of non-nuclear somatic histones during bovine spermiogenesis. *Biol. Reprod.* **71**, 1182–1194
- Vignali, G., Lizier, C., Sprocati, M.T., Sirtori, C., Battaglia, G. and Navone, F. (1997) Expression of neuronal kinesin heavy chain is developmentally regulated in the central nervous system of the rat. *J. Neurochem.* **69**, 1840–1849
- Vijayaraghavan, S., Stephens, D.T., Trautman, K., Smith, G.D., Khatra, B., da Cruz e Silva, E.F. and Greengard, P. (1996) Sperm motility development in the epididymis is associated with decreased glycogen synthase kinase-3 and protein phosphatase 1 activity. *Biol. Reprod.* **54**, 709–718
- Walden, P.D. and Cowan, N.J. (1993) A novel 205-kilodalton testis-specific serine/threonine protein kinase associated with microtubules of the spermatid manchette. *Mol. Cell. Biol.* **13**, 7625–7635
- Walden, P.D. and Millette, C.F. (1996) Increased activity associated with the MAST205 protein kinase complex during mammalian spermiogenesis. *Biol. Reprod.* **55**, 1039–1044
- Wang, R. and Sperry, A.O. (2008) Identification of a novel leucine-rich repeat protein and candidate PP1 regulatory subunit expressed in developing spermatids. *BMC Cell Biol.* **9**, 9
- Xia, C., Rahman, A., Yang, Z. and Goldstein, L.S. (1998) Chromosomal localization reveals three kinesin heavy chain genes in mouse. *Genomics* **52**, 209–213
- Yaffe, M.B., Farr, G.W., Miklos, D., Horwich, A.L., Sternlicht, M.L. and Sternlicht, H. (1992) TCP1 complex is a molecular chaperone in tubulin biogenesis. *Nature* **358**, 245
- Yang, J., Morales, C.R., Medvedev, S., Schultz, R.M. and Hecht, N.B. (2007) In the absence of the mouse DNA/RNA-binding protein MSY2, messenger RNA instability leads to spermatogenic arrest. *Biol. Reprod.* **76**, 48–54
- Yang, W.X. and Sperry, A.O. (2003) C-terminal kinesin motor KIFC1 participates in acrosome biogenesis and vesicle transport. *Biol. Reprod.* **69**, 1719–1729
- Yoshida, T., Ioshii, S.O., Imanaka-Yoshida, K. and Izutsu, K. (1994) Association of cytoplasmic dynein with manchette microtubules and spermatid nuclear envelope during spermiogenesis in rats. *J. Cell Sci.* **107**, 625–633
- Zhang, Y., Wang, R., Jefferson, H. and Sperry, A.O. (2007) Identification of motor protein cargo by yeast 2-hybrid and affinity approaches. In *Molecular Motors: Methods and Protocols* (Sperry, A.O., ed.), volume 392, pp. 97–116, Humana Press, Totowa, NJ
- Zou, Y., Millette, C.F. and Sperry, A.O. (2002) KRP3A and KRP3B: candidate motors in spermatid maturation in the seminiferous epithelium. *Biol. Reprod.* **66**, 843–855

Received 2 June 2009/30 October 2009; accepted 4 November 2009

Published as Immediate Publication 4 November 2009, doi:10.1042/BC20090091

Supplementary online data

TLRR (Irrc67) interacts with PP1 and is associated with a cytoskeletal complex in the testis

Rong Wang, Aseem Kaul and Ann O. Sperry¹

Department of Anatomy and Cell Biology, Brody School of Medicine at East Carolina University, Greenville, NC 27834, U.S.A.

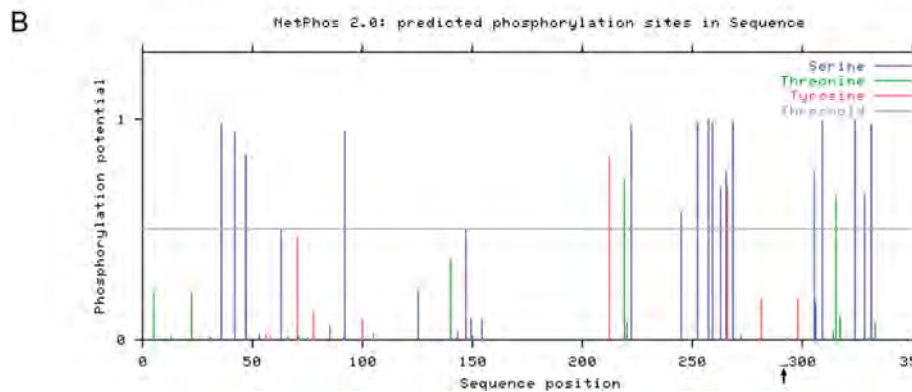
Figure S1 | TLRR sequence contains multiple potential serine phosphorylation sites

The TLRR amino acid sequence was analysed for the presence of phosphorylation sites using NetPhos 2.0 prediction software (Blom et al., 1999). **(A)** The sequence of TLRR is shown with serine residues predicted to have an extremely high probability of phosphorylation (prediction score >0.9) indicated in boldface. The PP1 consensus binding site is boxed. **(B)** A graphical illustration of phosphorylation sites along the TLRR polypeptide is shown with the N-terminus to the left of the graph (x-axis=sequence position). Predicted serine phosphorylation is shown in blue, threonine in green, and tyrosine in red with relative probability of phosphorylation indicated by the height of the bar (y-axis=phosphorylation potential). The relative position of the PP1-binding site is indicated with an arrow.

A

```

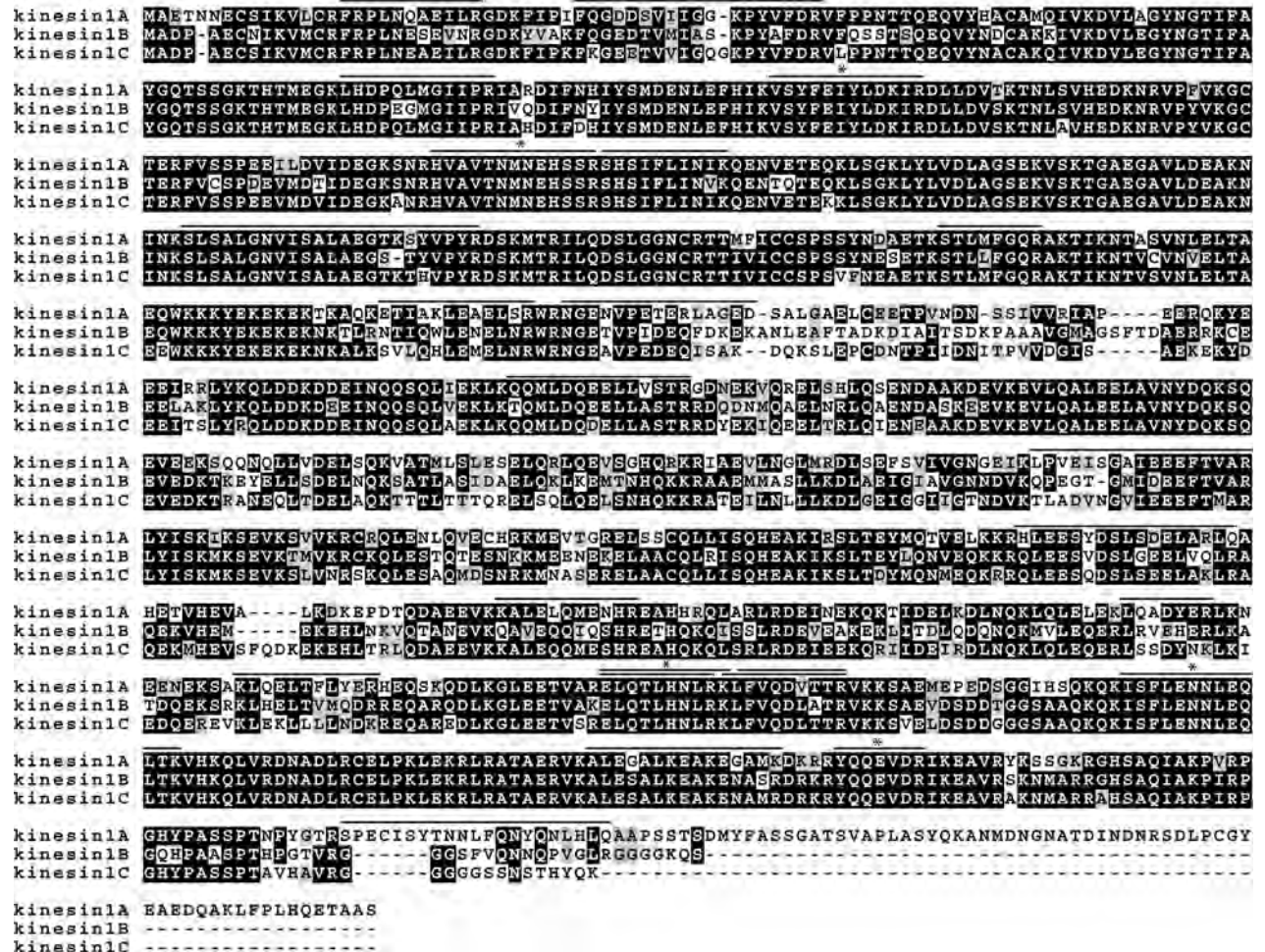
MVRLTVDLIAKNSNLKPRKEETLAQCLKKITHINFSDRNIDSIDDLSLCRNLSVLYLYDNRISQVTNLNYTTNLTHLYLQ 80
NNCISCIENLSSLKLEKLYLGGNYIAVIEGLELEELRELHVESQRLPLGKLLFDPRTLRSLAKSLSTLNISNNNIDD 160
IKDLEILENLNHLIAVDNQLMHVKDLELLKLMKLMKMDLNGNPVCLPKPYRDKLILTSKSLFELFDGKEIKDMERQFLM 240
NWKASKDAKKISKRRSRSEASNSYISNFETVHHIVPVYYPQVGKPKVLFPSDVQRYLVHGNASSKCSQEDKTTITEDI 320
GNLSLKESESSLTKNDIHEPHLLQNPVKVENLSEKKE 400
    
```



¹ To whom correspondence should be addressed (email sperrya@ecu.edu).

Figure S2 | Sequence alignment of kinesin-1 subfamily members with peptides identified by MALDI-TOF/TOF of the TLRR complex

Kinesin-1 subfamily members A–C were aligned with ClustalW2 software (Larkin et al., 2007). The 25 peptides identified by MALDI-TOF/TOF are indicated with black bars above the sequence with asterisks to denote the six peptides with sequence common to all three isoforms. The sequences of the remaining 19 peptides exactly match kinesin-1B and contain one or more mismatches to the other two isoforms. Black, identical residues; grey, similar residues; white, different residues.



TLRR is associated with a protein complex in spermatids

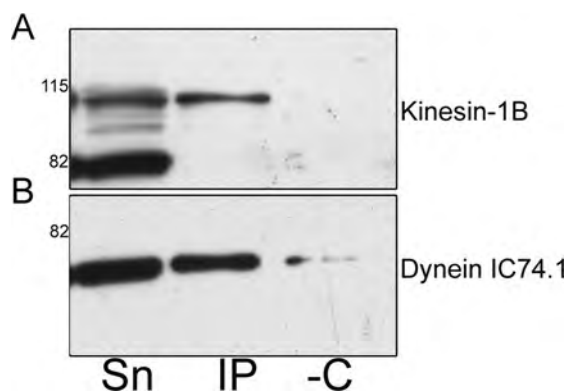
Table S1 | TLRR in 3T3 cells is associated with a protein complex containing cytoskeletal proteins and Hsps

Proteins purified by affinity chromatography from 3T3 cell lysate using a TLRR antibody are shown. The number of peptides and the percentage sequence coverage of each identified protein are indicated. Ddx5, DEAD box polypeptide 5.

Protein name	Protein ID	Number of peptides identified	% Sequence coverage
β -Actin	gi 49868	15	51
γ -Actin	gi 809561	15	51
β -Tubulin	gi 7106439	12	26
Heterogeneous nuclear ribonucleoprotein K	gi 74198765	7	22
Hsp90b	gi 40556608	12	20
Hsp70	gi 215260057	10	20
Heterogeneous nuclear ribonucleoprotein U	gi 160333923	17	19
Ddx5	gi 55562721	11	18
α -Tubulin	gi 202210	6	17
p100 co-activator	gi 6009521	12	14

Figure S3 | TLRR interacts with kinesin-1B and dynein in 3T3 cell lysate

The affinity-purified TLRR antibody bound to Sepharose beads, or non-specific normal rabbit IgG (-C), was incubated with 1.5–2 mg of testis lysate. Proteins unbound (Sn) or bound to the beads (IP) were separated by SDS/PAGE, transferred to a membrane, and probed with antibodies to the proteins indicated on the right: (A) kinesin-1B and (B) dynein IC 74.1. The migration of Benchmark prestained protein mass standards (Invitrogen) is indicated on the left.



References

- Blom, N., Gammeltoft, S. and Brunak, S. (1999) Sequence and structure-based prediction of eukaryotic protein phosphorylation sites. *J. Mol. Biol.* **294**, 1351–1362
- Larkin, M.A., Blackshields, G., Brown, N.P., Chenna, R., McGettigan, P.A., McWilliam, H., Valentin, F., Wallace, I.M., Wilm, A., Lopez, R. et al. (2007) Clustal W and Clustal X version 2.0. *Bioinformatics* **23**, 2947–2948

Received 2 June 2009/30 October 2009; accepted 4 November 2009

Published as Immediate Publication 4 November 2009, doi:10.1042/BC20090091